DOI: https://doi.org/10.68732/73269b3758b9402d

ISBN: 978-9989-2053-6-1

# Effect of rock matrix permeability on fluid-injection-induced hydro-mechanical coupled behaviour of rock discontinuities

A. Sainoki
*Kumamoto University, Kumamoto, Japan*
atsushi_sainoki@kumamoto-u.ac.jp
*0000-0003-2754-4801*

D. Asahina
*The National Institute of Advanced Industrial Science and Technology, Tsukuba, Japan*

N. Iwata
*Chuden Engineering Consultants Co.,Ltd, Hiroshima, Japan*

A. Schwartzkopff
*The University of Western Australia, Perth, Australia*

## Abstract

Fluid injection into rock masses and the associated hydro-mechanical coupled behaviour are of paramount importance in deep underground engineering projects. Although numerous studies have been undertaken to investigate the fluid behaviour in rock discontinuities, most of the studies neglect the possibility of fluid leakage to the surrounding rock matrix, which may lead toan overestimation of the risk for instability leading to shear failure and/or induced seismicity. To evaluate its influence, the present study conducted fluid injection experiment and simulation whilst varying the permeability of the rock matrix surrounding the discontinuity. The experiment employed rectangular parallelepiped rock specimens with a through-going discontinuity inclined at 60°. The experiment indicated the significant effect of the rock matrix permeability on the increase rate and peak value of the pore pressure in the discontinuity as well as the occurrence of slip. Specifically, when fluid is injected at the rate of 0.03 mL/min, slip occurs only for the intact specimen, whilst slip took place for the specimen heated at 500 °C at an injection rate of 0.3 mL/min, implying the existence of a threshold above which the discontinuity stability drastically decreases. This hydro-mechanical coupled behaviour was further confirmed through the numerical simulation, demonstrating the non-linear evolution of the pore pressure and shear displacement. This study provides important insights into the role of the rock matrix in the hydro-mechanical coupled behaviour of rock discontinuities and contributes to the improvement of evaluation methods for the risk of induced seismicity.

## Keywords

Induced seismicity, Near-discontinuity rock matrix permeability, Numerical simulation.

# 1 Introduction

Fluid injection-induced seismicity is associated with various engineering projects including enhanced geothermal system, carbon capture and storage, and hydraulic fracturing for destressing in deep underground mining (Sainoki, 2014; Ge and Saar, 2022). It has been attracting significant global attention due to the increasing depth and scale of these engineering projects. For example, during the 2017 EGS project in Pohang, fluid injection into the stimulated reservoir activated a previously stable fault, triggering a magnitude 5.4 earthquake that caused significant economic damage (Kim et al., 2023). This event became the second-largest recorded earthquake in South Korea, and because the country is generally regarded as a region of low seismic activity, the earthquake attracted considerable attention from both the scientific community and the government. The cause of injection-induced seismicity is primarily the reduction of the effective normal stress acting on discontinuities within a rock mass due to an increase in pore pressure. When the shear stress exceeds the reduced frictional resistance, shear failure occurs along the discontinuity. Such slip behavior can be classified into seismic slip or aseismic slip depending on the stability of the fracture system, the ambient stress state, infilling materials, the stiffness of the surrounding rock mass, and so forth. Furthermore, slip along discontinuities alters the hydraulic properties of fractures (Zhao et al., 2025) and surrounding damage zones, thereby influencing fluid migration and pore pressure distribution within the reservoir. Thus, in-depth investigation of the mechanisms governing the evolution of induced seismicity and its consequences is required for ensuring the sustainable and safe operation in such subsurface engineering projects.

Significant experimental and numerical efforts have been devoted to understanding the influence of fluid injection on the mechanical and hydraulic behaviour of rock discontinuities. These studies have provided valuable insights into various physical phenomena, including the influence of injection rate on slip occurrence (Hutka et al., 2023), slip-induced permeability evolution of rock discontinuities, and the effect of surface asperities (Ji et al., 2023). Some studies indicated the strong influence of microscopic fracture distributions within a rock matrix on the mechanical behaviour of rock discontinuities, especially for rocks with a relatively high matrix permeability (Schwartzkopff et al., 2021). Hence, when fluid injection is performed into such rock discontinuities surrounded by permeable rock matrices, it is essential to evaluate their influence on the evolution of pore pressure along discontinuities and the occurrence of slip. In particular, clarifying and quantifying the relationship among matrix permeability, pore pressure evolution, and discontinuity slip behaviour remains an important research challenge, owing to difficulties in controlling the permeability of the rock matrix surrounding a discontinuity.

To address this issue, in the present study, we performed laboratory-scale fluid injection experiments while varying the permeability of near-discontinuity rock matrix by inducing thermal damage to granite specimens in an oven before the injection experiment. Subsequently, to verify the experiments and quantify the influence of the rock matrix with enhanced porosity, numerical simulations were performed within the framework of the Distinct Element Method (DEM) by performing hydro-mechanical coupled simulation whilst considering the fluid leakage to the surrounding rock matrix. The objective of the present study is to identify key parameters controlling the coupled hydro-mechanical response. The findings obtained from this study are expected to contribute to improving predictive methodologies for fluid injection-induced seismicity and to advancing induced seismicity risk assessment for subsurface engineering applications involving fluid injection into rock masses.

# 2 Fluid injection experiment

## 2.1 Specimen preparation

Rectangular prism specimens of Inada granite were used in the experiments. The specimens were cut at an angle of 30° to the longitudinal axis using a rock cutter to create a precut surface, as shown in Fig.1. Subsequently, the precut surface was polished with #400 abrasive paper using a rotary polishing machine. Of the pair of cut specimens, one specimen was drilled with a through-going injection hole ($\varphi$ = 2 mm) using an ultrasonic drill. This injection hole enabled direct water supply from the syringe pump injection line to the precut surface.

In total, three types of specimens were prepared while varying the degree of microcrack density in the rock matrix, namely I-R, I-300, and I-500. I-R denotes an intact specimen prepared at room temperature without any damage, while the other two specimens (I-300 and I-500) were heated in an oven to generate microcracks, thereby simulating a damage zone with a high permeability. It is known

that the aperture of microcracks in Inada granite increases with increasing maximum thermal history temperature. In this study, specimens were heated at 300°C (I-300) and 500°C (I-500) for 20 minutes.

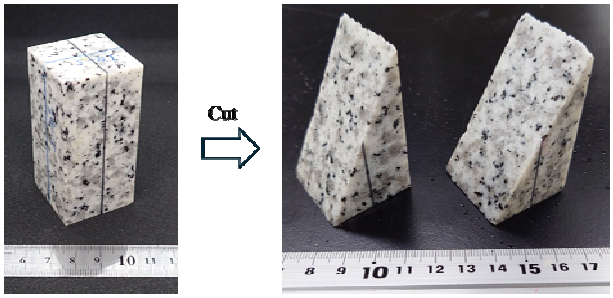



Fig.1 Intact specimens of Inaga granite, with a precut surface, cut at an angle 30° to the longitudinal axis.

### 2.2 Overview of the experimental apparatus and procedure

The experiments were conducted using a large-scale triaxial testing machine and two syringe pumps. The triaxial testing machine is capable of simulating underground stress conditions by controlling axial loading and confining pressure applied in all directions. In addition, the two syringe pumps enabled control of water flow from both the upstream and downstream sides of the specimen. After being fully saturated, the granite specimen was covered with a transparent silicone jacket and installed in the triaxial testing machine with flow lines connected to the upper and lower end pieces. LDTs were attached in both the longitudinal and lateral directions of the specimen to measure deformation.

The experimental procedure is as follows; (a) The specimen was installed in a pressure vessel, and a confining pressure of 10 MPa was applied uniformly to the entire lateral surface of the specimen; (b) The pore pressure within the specimen was controlled at a constant pressure of 1 MPa; (c) Axial load was applied in the longitudinal direction of the specimen until the stress state reached a critical condition determined by Mohr-Coulomb failure criterion, and then the piston displacement was fixed; (d) While maintaining the downstream side at a constant pressure of 1 MPa, water was injected from the upstream side at a constant flow rate to increase the pore water pressure along the discontinuity (precut surface); (e) The increase in pore water pressure induced slip along the precut surface of the rock specimen;(f) The flow rate was changed, and steps (b)–(e) were repeated.

## 3 Numerical simulation

### 3.1 Numerical model

Fig. 2 depicts the numerical model replicating the specimen used for the fluid injection experiment. As shown in Fig. 2(a), the dimensions of the numerical model are 34 mm in width, 34 mm in length, and 66 mm in height, which are consistent with specimens for the experiment. The through-going discontinuity, which is a precut surface in the case of the experiment, dips at 60°. Fig. 2(b) shows a through-going discontinuity simulated in the model, corresponding to the precut surface shown in Fig. 1. The boundary conditions and initial conditions were identical to the fluid injection experiments.

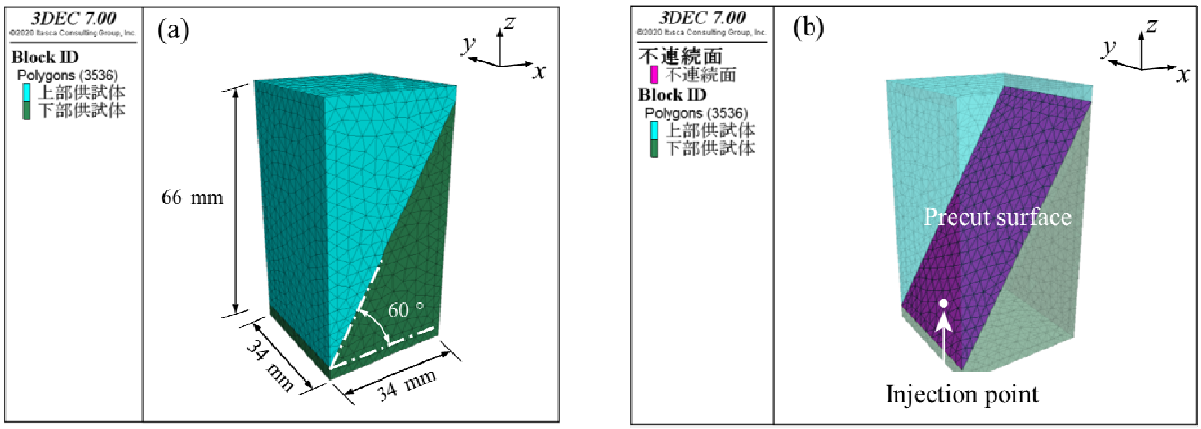



Fig. 2 Numerical model: (a) Isometric view of the numerical model replicating the specimen used for the injection experiment, (b) Perspective view showing a through-going discontinuity in the numerical model and a fluid injection point.

### 3.2 Input parameters

The elastic modulus of the specimen and Poisson's ratio were assumed to be 60 GPa and 0.2, respectively, considering a reasonable range of elastic parameters for granite. The density was set at 2600 kg/m$^3$. The hydraulic permeabilities of I-R, I-300, and I-500 were estimated at $1.0\times10^{-11}$ m/s, $3.0\times10^{-10}$ m/s, $1.0\times10^{-8}$ m/s, respectively, by performing permeability tests on specimens that had undergone thermal-induced damage. Regarding the porosity of the specimens, the values were estimated as 0.01, 0.011, and 0.019 for I-R, I-300, and I-500, respectively, from CT scanning and image analysis, as shown in Fig. 3. The CT scanning was performed using a SkyScan2214 system under the conditions of 100 kV, 75 µA, and an exposure time of 7000 ms, which resulted in a scanning time of approximately 21 hours and a spatial resolution of 6 µm.

Regarding the parameters of the discontinuity to which fluid is injected during the simulation, the following parameters were used; the normal and shear stiffnesses were assumed to be 60 GPa/m and 20 GPa/m, respectively; the friction angle was set at 30°, assuming that the value remains unchanged during slip; the cohesion was set at 0° as it is a precut surface; and the hydraulic aperture of the discontinuity was assumed to be 1.5 µm.

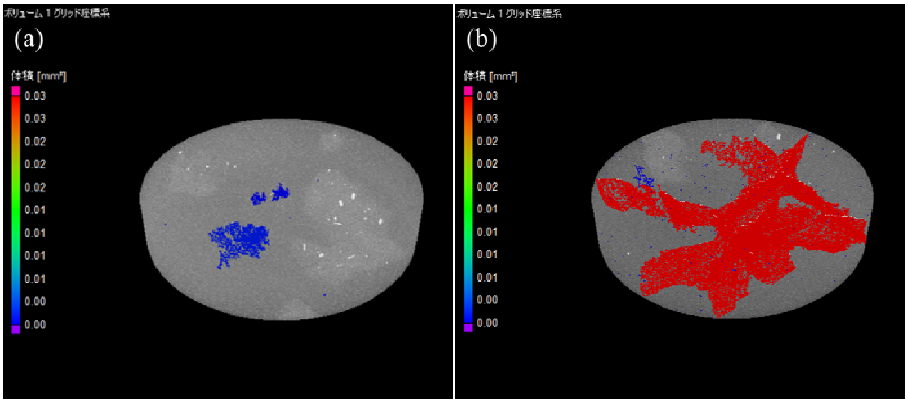



Fig. 3 3D image reconstructed from CT scanning with nano-focused X-ray CT scanner and identification of fracture network based on image analysis: (a) I-300, (b) I-500.

## 4 Results and discussion

### 4.1 Experimental results

Fig. 4(a) shows changes in shear stress, lateral displacement, and pore pressure during the injection test at an injection rate of 0.03 mL/min. As explained in the previous section, the axial load is first increased until the stress state reaches almost the critical condition, which is followed by fluid injection at a constant injection rate. As can be seen in Fig. 4(a), after the shear stress reaches the peak value, the fluid injection increases the pore pressure. As the loading plate is fixed during the injection, the shear stress gradually decreases due to relaxation until 500 s. Then, it is to be noted that a sudden reduction of shear stress takes place, as indicated by "slip" in the figure. At the moment, the shear stress suddenly decreases with an increase in the lateral displacement, thus implying the occurrence of slip. The shear stress reduction would be the combined effect of continuously increasing pore pressure and slip-weakening behaviour. Subsequently, the fluid injection is terminated, and the axial load is repeatedly increased so that the stress state acting on the precut surface reaches almost the critical condition. Fig. 4(a) includes results from three injection tests, clearly showing the slip event for each case and thereby demonstrating the reproducibility of the tests. Especially, the most noticeable shear stress reduction took place during the third injection test.

Fig. 4(b) shows results for the three types of specimens, i.e., I-R, I-300, and I-500, when fluid was injected at a constant rate of 0.03 mL/min. As shown in Fig. 4(a), for each specimen, the fluid injection test was repeated. Accordingly, representative results are shown in Fig. 4(b). It is to be noted that as explained previously, the shear stress reduction taking place after fixing the displacement of the loading plate in the axial direction is attributed to relaxation, which is not related to the occurrence of slip. In addition, the timing at which fluid injection was initiated differs among the cases. As the shear stress almost remains stable when the injection was started, the timing does not exert any influence on the result. Given these considerations, the result clearly demonstrates the influence of the rock matrix

permeability in that the shear stress shows a sudden drop during the fluid injection-induced evolution of pore pressure only for I-R. As can be seen, the shear stress starts to decrease 500 s after the onset of the injection test in the case of I-R, whilst the shear stress remains almost the same for the other cases. In addition, the pore pressure evolution history remarkably differs among the specimens. The linear increase in pore pressure in the case of I-R implies that the low-permeable rock matrix hinders the permeation of fluid into the surrounding region. In contrast, in the case of I-300 and I-500, the pore pressure moderately increases, indicating that the microcracks generated when heated in an oven facilitate the filtration of injected fluid into the surrounding rock matrix, so that the increase in pore pressure was controlled. These results provide valuable insights into the role of hydraulic characteristics of rock matrices surrounding rock discontinuities in the occurrence of injection-induced slip behaviour and resultant seismic events.

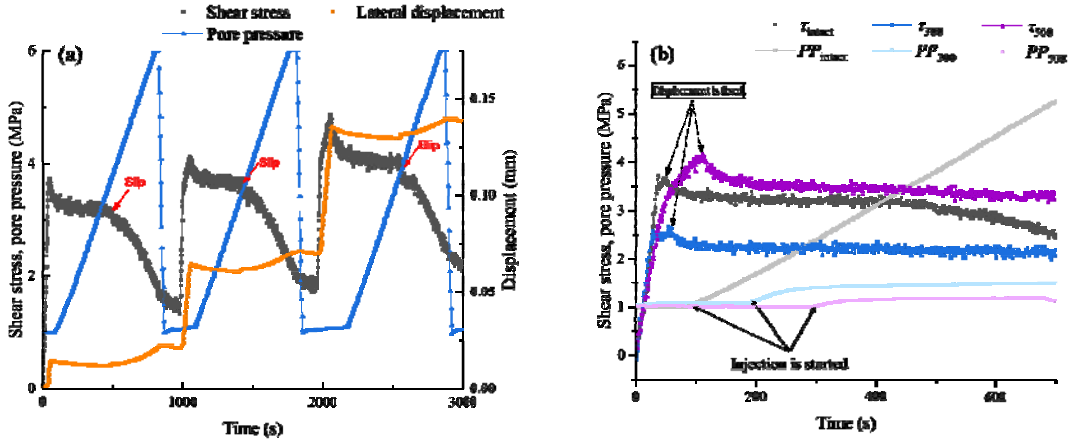



Fig. 4 Experimental results: (a) Results for IR at a fluid injection rate of 0.03ml/min, and (b) Results for I-R, I-300, and I-500 at a fluid injection rate of 0.03 mL/min.

## 4.2 Numerical simulation results

Fig. 5(a) shows the change in pore pressure over time during fluid injection obtained from the numerical simulation. In terms of pore pressure increment at 300 s after the initiation of fluid injection, the numerical simulation results are comparable to those in Fig. 4(b). For instance, for the experiment, the pore pressure increases by 0.19 MPa in the case of I-500, while the numerical simulation resulted in an increase of approximately 0.20 MPa. Comparable results were also obtained for the other cases, thus verifying the numerical simulation to some extent. However, there is a discrepancy between the experiment and numerical simulation in that the pore pressure gradient differs. It appears that pore pressure increases more rapidly and drastically in the numerical simulation compared to the experiment, irrespective of the degree of thermal-induced damage. It is presumed that this discrepancy is attributed to the location where the pore pressure is measured. In the case of the experiment, pore pressure is measured at the injection tube outside the pressure vessel, whilst the numerical simulation does not consider either the injection tube or the hole drilled in the lower block to inject fluid into the precut surface, and the pore pressure is monitored at the injection point on the discontinuity directly during the simulation. It is thus plausible to assume that the hydro-mechanical coupled behaviour of the hole in the lower block exerted an influence on the pore pressure measured at the tube.

Fig. 5(b) shows pore pressures at 200 s after the initiation of fluid injection for different injection rates. As shown, the response significantly differs among the specimens. More specifically, the intact rock matrix (I-R) results in a higher increase in pore pressure when the injection rate was increased. This result is deemed reasonable because the impermeable rock matrix controls fluid leakage from the discontinuity, yielding a rapid increase in pore pressure on the discontinuity. The contour image shown in Fig. 5(b) corresponds to the pore pressure distribution on a cross-section for I-500 at an injection rate of 0.3 mL/min. As shown, the fluid migrates to the rock matrix surrounding the discontinuity, thereby controlling pressurization at the injection point. The purple colour on the discontinuity corresponds to a slipping region.

These results imply that the permeability of the rock matrix surrounding the discontinuity can play a critical role in the occurrence of instability, i.e., slip can be controlled when an injection rate is properly controlled considering the permeability of the surrounding rock matrix.

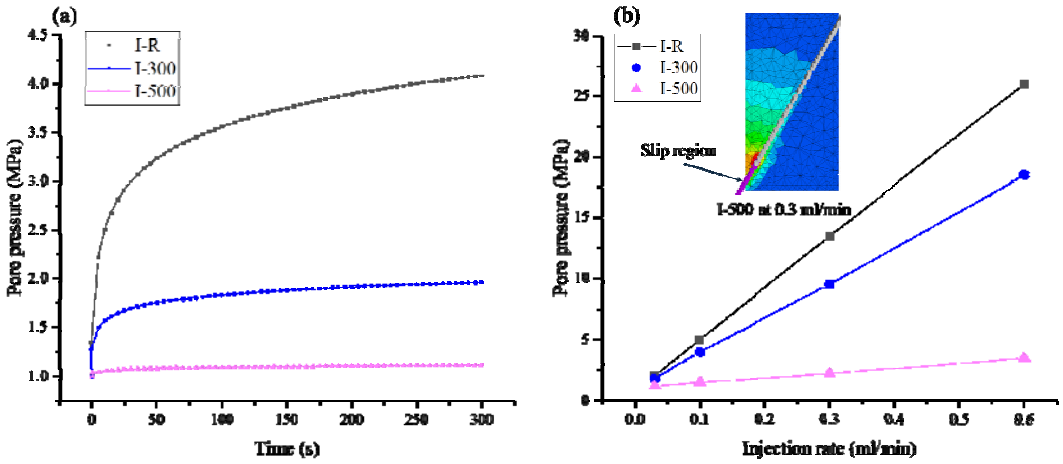



Fig. 5 Pore pressure at the injection point: (a) Pore pressure change during injection, (b) Pore pressure at 200 s for different fluid injection rates.

## 5 Conclusions

The present study investigated the effect of the discontinuity-surrounding rock matrix permeability on pore pressure evolution and slip occurrence on the discontinuity during fluid injection. To this end, fluid injection experiments were performed by preparing specimens containing a through-going discontinuity. The rock matrix permeability was varied among the specimens by inducing different degrees of thermal damage in an oven prior to the experiment. The thermally induced microfracture network was quantified with nano-focused X-ray CT imaging. Subsequently, fluid injection experiments were carried out, which clearly indicated that when fluid injection rate is 0.03 mL/min, the pore pressure increase rate was sufficiently low to control the occurrence of slip for the specimen that had undergone severe thermal damage, whereas for the intact specimen without thermally induced damage pore pressure rapidly increased, causing slip along the discontinuity. These finding simply show that the rock matrix permeability plays a pivotal role in the pore pressure evolution along the discontinuity and the occurrence of instability. The influence of the fluid leakage to the surrounding rock matrix on the occurrence of slip along the discontinuity was further quantified through numerical simulations after verifying the numerical model. Based on these findings, it can be concluded that fluid injection-induced seismicity can be mitigated by properly controlling fluid injection rate whilst considering the permeability characteristics of the rock matrix surrounding discontinuities.

## References

Sainoki, A.,Mitri, H. S. (2014). Dynamic behaviour of mining-induced fault slip. International Journal of Rock Mechanics and Mining Sciences, *66*, 19-29.

Ge, S., Saar, M. O. (2022). Induced seismicity during geoenergy development—A hydromechanical perspective. Journal of Geophysical Research: Solid Earth, 127(3), e2021JB023141.

Kim, T., Park, J. H., Yu, E. (2023). Seismic fragility of low-rise piloti buildings based on 2017 Pohang earthquake damage. Journal of Building Engineering, 76, 107032.

Zhao, W., An, M., Dal Zilio, L., Zhao, L., Zhu, H., Shen, X., Gan, Q., Zhang, F., Elsworth, D. (2025). Coupled evolution of seismicity and permeability in fault zones. Communications Earth & Environment, 6(1), 918.

Hutka, G. A., Cacace, M., Hofmann, H., Zang, A., Wang, L.,Ji, Y. (2023). Numerical investigation of the effect of fluid pressurization rate on laboratory-scale injection-induced fault slip. Scientific Reports, 13(1), 4437.

Ji, Y., Zhang, W., Hofmann, H., Cappa, F., & Zhang, S. (2023). Fracture permeability enhancement during fluid injection modulated by pressurization rate and surface asperities. Geophysical Research Letters, 50(18), e2023GL104662.

Schwartzkopff, A. K., Sainoki, A., Elsworth, D. (2021). Numerical simulation of mixed aseismic/seismic fault-slip induced by fluid injection using coupled X-FEM analysis. International Journal of Rock Mechanics and Mining Sciences, 147, 104871.